Int. J. Electrochem. Sci., 11 **(2016)** 2197 - 2204

International Journal of ELECTROCHEMICAL SCIENCE
www.electrochemsci.org

Short Communication

Sol Gel Synthesized Zinc Oxide Nanorods on Single And Co-doped ZnO Seed Layer Templates: Morphological, Optical and Electrical Properties

Ruziana Mohamed[1,2,3,*], *Jalal Rouhi*[1,2], *Mohd Firdaus Malek*[1,2], *Ahmad Syakirin Ismail*[1], *Salman A.H Alrokayan*[5], *Haseeb A. Khan*[5], *Zuraida Khusaimi*[2,4], *Mohamad Hafiz Mamat*[1,2], *Mohamad Rusop Mahmood*[1,2]

[1]NANO-ElecTronic Centre, Faculty of Electrical Engineering, Universiti Teknologi MARA, 40450 Shah Alam, Selangor, Malaysia
[2]Centre of Nanoscience and Nanotechnology (NANO-SciTech Centre), Institute of Science, Universiti Teknologi MARA, 40450 Shah Alam, Selangor, Malaysia
[3]Faculty of Applied Sciences, Universiti Teknologi MARA Pahang, 26400 Bandar Tun Razak Jengka, Pahang, Malaysia
[4]Faculty of Applied Sciences, Universiti Teknologi MARA, 40450 Shah Alam, Selangor, Malaysia
[5]Department of Biochemistry, College of Science, King Saud University (KSU), Riyadh 11451, Kingdom of Saudi Arabia
[*]E-mail: ruziana12@gmail.com

Received: 16 June 2015 / *Accepted:* 5 September 2015 / *Published:* 1 February 2016

Highly ordered and uniform vertical ZnO nanorod arrays were synthesized by a facile and low-temperature sol–gel method using two different seed layers [i.e., Mg-doped ZnO (MZO) and Al,Mg-doped ZnO (AMZO)] and deposited by spin coating technique. Field-emission scanning electron microscopy images confirmed that vertical, denser, and orderly ZnO nanorods are grown on AMZO seed layer compared with that synthesized on MZO seed. UV–visible spectra indicated that Al and Mg additives could significantly enhance the optical transparency and induce a blueshift in optical band gap of ZnO films. The electrical property shows that ZnO nanorods grown on AMZO seed have lower resistivity of 2.30 Ω cm than that on MZO seed (7.67 Ω cm). The electrical conductivity of ZnO films grown on co-doped seed layer could be tailor and this might be effectively inducing the geometric growth of ZnO films by sol–gel.

Keywords: ZnO nanorods; Seed layer; Surface morphology; Optical properties; Electrical properties

1. INTRODUCTION

Many researchers have focused on synthesis of one-dimensional (1D) nanostructures to enhance the performance of electronic devices. For instance, 1D oxide nanostructures such as

nanorods or nanowires have shown fast response, stability, and high sensitivity in gas sensors [1, 2] and improved light trapping efficiency in UV photodetectors [3, 4]. Zinc oxide (ZnO) nanorods are promising materials to use in electronic devices because of its thermal and chemical stability and high conductivity properties [5-7]. Several efforts have been made to improve the growth processes for such nanostructures appropriate for their application. Investigations on the preparation of ZnO thin films have focused not only in changing optical and morphological properties but also in improving electrical properties to meet the demands of electronics applications. The properties of ZnO films may be improved by doping. However, single doping is insufficient to improve the properties of ZnO thin films simultaneously, thus, the use of co-doping metals [8]. Magnesium and aluminum metal elements are widely used in single doping to alter the optical and electrical properties of ZnO films. Mg^{2+} substitution in ZnO will not contribute extra charge carriers. Nevertheless, Mg doping may enhance electron scattering and grain boundary barrier effects [9, 10]. By contrast, Al doping may increase charge carriers in ZnO films owing to the extra ion charge of Al element [11, 12]. Sol–gel immersion techniques offer a better preparation method to grow ZnO nanostructure films in terms of cost effectiveness, simplicity, and operation at low temperature [4, 13, 14]. However, several parameters need to be considered in using this technique. Recently, ZnO nanostructure thin films grown on different seed layer template have been widely investigated. Lee et al. [15] reported that the density, crystallization, and alignment of ZnO nanorod growth on ZnO and Argentum (Ag) doped ZnO seed changed with metal doping of ZnO seed layer. Wahid et al. [16] investigated the effect of ZnO seed annealed at different temperature on growth of ZnO nanorods and obtained the lowest resistivity of 6.67×10^3 Ω cm. B. Ikizler and S.M. Peker [17] prepared vertical ZnO nanorods with good crystallinity on different thickness of ZnO seed. They found that the average thickness of ZnO nanorods is 4 μm on 220 nm to 340 nm thick seed layers. Although there are researchers who are studying the effects of Al and Mg doping of ZnO, but research was only focused on the formation of nanoparticles [8, 9, 18]. The new approach was done in this study where we used the Al and Mg co-doped ZnO as a seed layer to grow the ZnO nanorods. Usually, ZnO nanorod was grown on ZnO or single doped ZnO seed such as Al doped ZnO seed [15-17, 19]. In the current study, we investigated the effects of two different ZnO seed layers (i.e., single and co-doped) prepared by sol–gel spin coating on the optical, morphological, and electrical conductivity properties of ZnO nanorods.

2. MATERIALS AND METHODS

Sol–gel spin coating method was used to prepare doped and co-doped ZnO seed layers on glass substrate. First, the glass substrate was cleaned using acetone, methanol, and deionized (DI) water for 10 m. For seed layer preparation, 2-methoxyethanol was dissolved with 0.4 M zinc acetate dehydrate [$Zn(CH_3COO)_2{\cdot}2H_2O$, 99.5%, Merck] as a precursor, 0.4 M monoethanolamine ($C_2H_7N_{14}$, 99.5%, Aldrich) as a stabilizer, and 0.012 M magnesium acetate tetrahydrate ($C_4H_6MgO_4{\cdot}4H_2O$) and 0.004 M aluminum nitrate nonahydrate [$Al(NO_3)_3{\cdot}9H_2O$, 98%, Analar] as dopant sources. The mixed solutions were heated and stirred at 80 °C for 3 h and aged at room temperature for 24 h to obtain homogeneous solutions. The solutions were dropped 10 times on glass substrate with a speed of 3000 rpm for 60 s.

After deposition process, the samples were preheated at 150 °C for 10 m in ambient atmosphere to remove the solvent. The deposition process was repeated for five times. The samples were then annealed at 500 °C for 1 h in a furnace. The ZnO nanorods arrays were grown on the seed layer using sol–gel immersion method. 0.1 M zinc nitrate hexahydrate [$Zn(NO_3)_2 \cdot 6H_2O$, 98% purity, Systerm] and 0.1 M hexamethylenetetramine ($C_6H_{12}N_4$, 99% purity, Aldrich) were used as precursor and stabilizer, respectively. All of the chemical materials were dissolved in distilled water and sonicated in ultrasonic water bath for 30 min (Hwasin Technology Powersonic 405; 40 kHz) at 50 °C. The mixed solution was then stirred and aged for 3 h at room temperature. The glass substrate coated with seed layer was then placed on the bottom of the vessels and the mixed solution was poured into the vessels with volume capacities of 100 ml. After that, the sealed vessels were immersed in a hot water bath at 95 °C for 30 min. After immersion, ZnO nanorods films were rinsed with DI water and dried in a furnace at 150 °C for 10 m. Finally, the samples were annealed at 500 °C for 1 h under ambient conditions. The optical and morphological properties were investigated by UV–visible spectroscopy (Cary 5000) and field-emission scanning electron microscopy (FESEM, JSM-7600F). Electrical properties were measured using a two-probe system (Advantest R6243).

3. RESULTS AND DISCUSSION

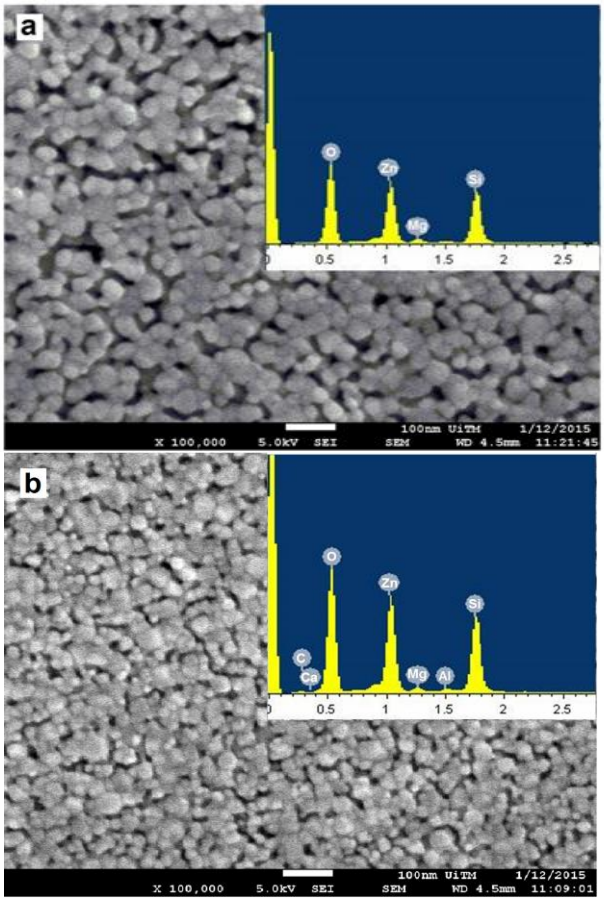

Figure 1. FESEM images and EDX results of the ZnO nanostructures deposited on glass substrate (a) Mg doped ZnO (b) Al and Mg co-doped ZnO.

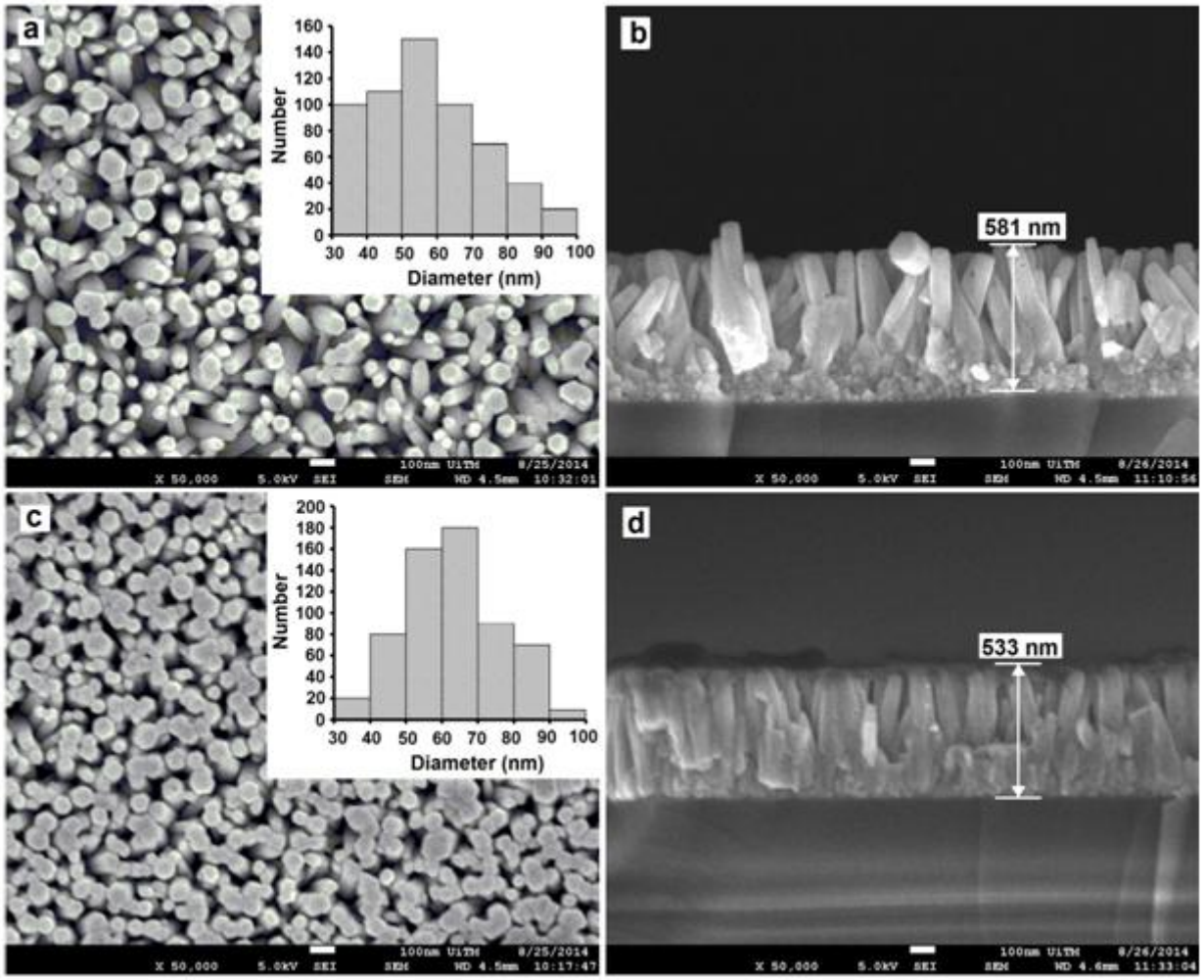

Figure 2. FESEM images, diameters distribution of ZnO nanorod and cross sectional area for ZnO nanarod on (a-b) MZO seed (c-d) AMZO seed.

The FESEM images and EDX results for MZO and AMZO seed layers are shown in Figures 1a and 1b. The particles for AMZO seed are more compact than MZO seed with less space between particles. The composition of Al, Mg, Zn, and O as elementary components in MZO seed and AMZO was determined based on the EDX data. Figure 1 confirms the presence of Mg and Al elements in ZnO thin films.

Figures 2a-2d show the FESEM images of ZnO nanorods films grown on MZO and AMZO seed layers. The ZnO nanorod growth appears as hexagonal wurtzite structure. The growth of ZnO nanorods on an AMZO seed layer is denser, orderly, and more vertically aligned compared with those on MZO thin film. Given that Mg^{2+} with ionic radius of 0.065 nm is almost similar to Zn^{2+} with ionic radius of 0.072 nm, substitution of Mg into ZnO lattice near or in boundary reduced the growth of nanoparticles and decreased the crystallite size [20]. However, doping with Mg together with Al^{3+} with ionic radius of 0.053 nm created simultaneous reaction and induced the change of crystallite size. Thus, an AMZO film has smoother, more homogenous, and more compact surface [8] than singly doped ZnO. Therefore, the distribution growth of ZnO nanorods on AMZO seed is more uniform than

those on MZO seed layer. The compact and homogenous surface of ZnO nanorod structure will influence to the sensing properties due to large surface area and suitable to be used for sensor application [5, 21]. The cross section images show that the thickness of the nanorods is approximately 581 nm and 533 nm on MZO and AMZO seed layers, respectively.

The inset in Figure 2a indicates the nanorod diameter distribution on the basis of the FESEM image. The diameter of the ZnO nanorods grown on MZO ranges from 30 nm to 100 nm, in which more than 80% of them have a diameter of 30–60 nm. The average diameter size of ZnO nanorod grown on MZO is 66.6 nm, which is smaller than that on AMZO seed layer (73.9 nm). The disparity of the nanorod width is believed to be caused by the inhomogeneous sizes of ZnO seed preformed on the substrates. Although the diameter distribution for ZnO nanorod grown on MZO seed is relatively small, its thickness is higher than that of nanorods grown on AMZO seed. Based on the aspect ratio analysis between length and diameter of ZnO nanorods, growth on AMZO seed has smaller value of 7.21 compared with 8.72 on MZO seed.

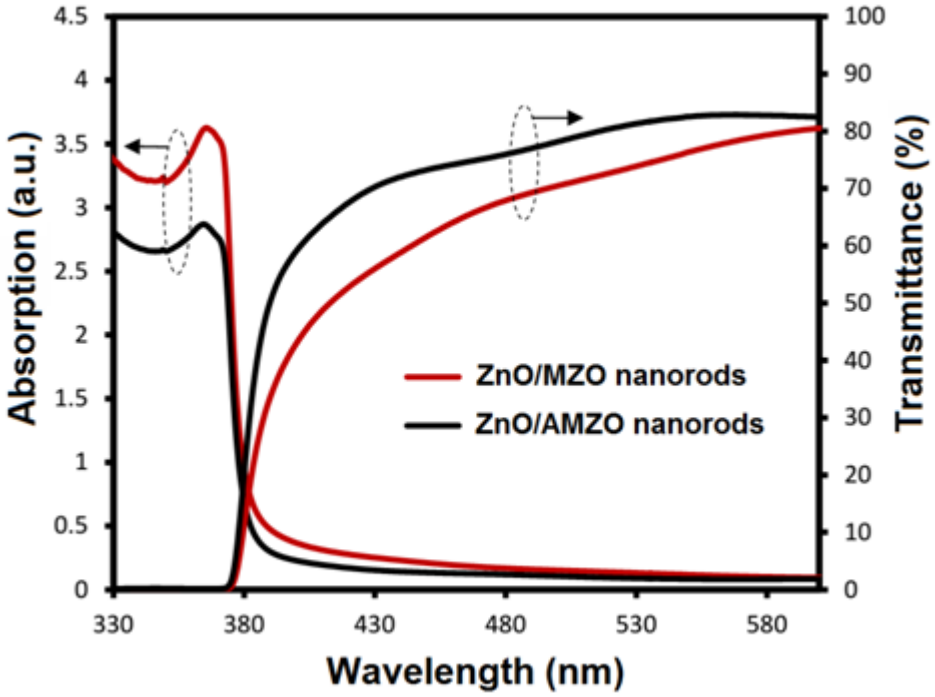

Figure 3. Transmittance and absorption peak of ZnO nanorod growth on different seed layer template.

Figure 3 shows the room-temperature optical transmittance and absorbance spectra of the ZnO nanorods grown on MZO and AMZO. The average transparency in the visible region (400–600 nm) for both ZnO thin films is more than 70%. ZnO/AMZO nanorods have higher transmittance than the ZnO nanorods deposited on MZO seed layer**.** The increase in transmittance spectrum might be related to well-aligned nanorod arrays in which more UV light is trapped and transmitted inside the thin film [4, 22]. FESEM images show that many ZnO nanorod arrays grew vertically towards *c*-axis from substrate for AMZO seed. The transmittance spectrum band edge of ZnO/AMZO nanorods was shifted towards lower wavelength which can be attributed to the optical confinement effect caused by the

nanorod geometry [15]. The ZnO thin films have high absorption properties in the UV region (<400 nm) wavelength. The optical band gap energy could be obtained based on Equation 1 [11]:

$$\alpha h\nu = A(h\nu - E_g)^{1/2} \quad (1)$$

where α is absorption coefficient, hν is photon energy, and A is a constant. The value of energy band gap was estimated around 3.66 and 3.78 eV for thin film grown on MZO and AMZO seed layers, respectively. The results show that the peak absorption of a thin film grown on AMZO seed layer has a blueshift compared with that grown on MZO seed layer. Normally, a blueshift of the absorption peak and enhancement of energy band gap for the thin film grown on the AMZO seed is attributed to an increase in the concentration of electrons, which is also known as the Burstein–Moss effect [11, 19].

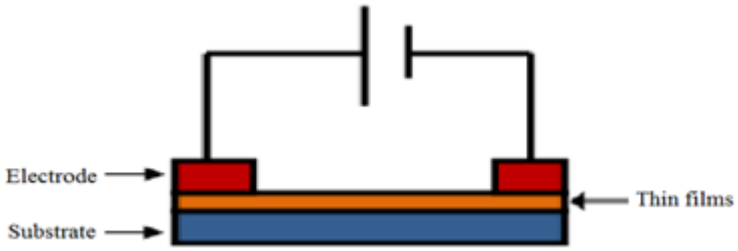

Figure 4. Configuration of I-V measurement using two point probe system.

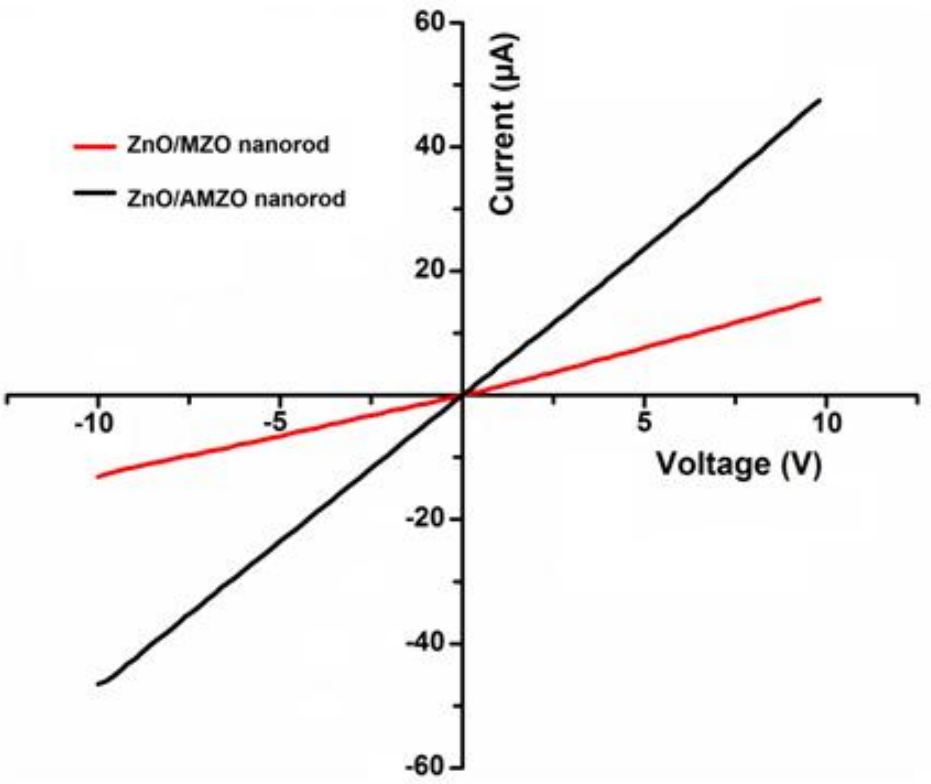

Figure 5. Characteristics of I-V measurement using two point probe system.

The configuration for current-voltage (I-V) measurement was shown in Fig. 4. In this study, 60 nm gold (Au) electrode was deposited on the thin film samples. The two points probe was used to measure the electrical properties of the thin films. Figure 5 shows the (I–V) characteristics of the ZnO nanorod films prepared on AMZO and MZO seed layer templates. The I–V curves were obtained using a two-probe measurement system in ambient illumination. Results show good ohmic contacts between Au metal and ZnO nanorod films and they increase proportionally in current to the supplied voltage. As shown in Fig. 4, the electrical properties of ZnO films grown on AMZO seed layer have higher values than those on the MZO thin film.

The ZnO nanorod grown on a AMZO showed a lower resistivity value (2.30 Ω cm) than that grown on MZO seed layer (7.67 Ω cm), which can be ascribed to the improvement of the carrier concentration in ZnO films by co-doping rather than by single doping the seed layer. The conductivity enhancement of ZnO/AMZO nanorods is attributed to the geometrical morphologies of ZnO nanorods that influence charge carriers. The uniformly distributed and compact ZnO nanorods arrays provide large surface area and less grain boundary effect that lead to enhanced carrier mobility. Thus this condition is useful for sensor application to improved the sensor performance [23]. Furthermore, co-doping with Al increased the extra charge and improved the electrical conductivity properties of ZnO films [4, 11, 24].

4. CONCLUSIONS

ZnO nanorods films were successfully grown on two different seed layer templates using sol–gel spin coating-immersion method. The optical properties of both ZnO thin films indicate that nanorods grown on AMZO seed have higher transmittance than those grown on MZO seed. FESEM images show that ZnO nanorods on AMZO are well-oriented and dense, attributing to the particle size and density of the seed layer. Electrical characterization shows that the resistivity of ZnO nanorods film is dependent on morphology, size, and growth orientation. These findings demonstrate that the co-doped seed layer has beneficial effects on ZnO nanorod growth by improving the electrical conductivity, which is suitable for sensor application.

ACKNOWLEDGEMENT
The author would like to acknowledgment to Ministry of Higher Education (MOHE) for financial support and also to Research Management Institute (RMI) for their support through the project the Long-Term Research Grant Scheme for Nanostructures, Nanomaterials and Devices for Fuel Cells and Hydrogen Production (600-RMI/LRGS 5/3 (3/2013). Appreciation was given to the Research Chair of Targeting and Treatment of Cancer Using Nanoparticles, Deanship of Scientific Research, King Saud University, Riyadh, Kingdom of Saudi Arabia for the Research Collaboration and Support.

References

1. D. Calestani, M. Zha, R. Mosca, A. Zappettini, M. Carotta, V. Di Natale, and L. Zanotti, *Sens. Actuators. B,* 144 (2010) 472-478.

2. C. Xie, L. Xiao, M. Hu, Z. Bai, X. Xia, and D. Zeng, *Sens.Actuators B,* 145 (2010) 457-463.
3. M.-Y. Chuang, H.-C. Yu, Y.-K. Su, C.-H. Hsiao, T.-H. Kao, C.-S. Huang, Y.-C. Huang, J.-J. Tsai, and S.-L. Wu, *Sens. Actuators B,* 202 (2014) 810-819.
4. M. H. Mamat, Z. Khusaimi, M. Z. Musa, M. F. Malek, and M. Rusop, *Sens. Actuators A,* 171 (2011) 241-247.
5. M. Bagheri, N. F. Hamedani, A. R. Mahjoub, A. A. Khodadadi, and Y. Mortazavi, *Sens. Actuators B,* 191 (2014) 283-290.
6. C. M. Chang, M. H. Hon, and I. C. Leu, *Sens. Actuators B,* 151 (2010) 15-20.
7. J. Chen, J. Li, J. Li, G. Xiao, and X. Yang, *J. Alloys Comp,* 509 (2011) 740-743.
8. D. Fang, K. Lin, T. Xue, C. Cui, X. Chen, P. Yao, and H. Li, *J. Alloys Comp.*, 589 (2014) 346-352.
9. L. Duan, X. Zhao, Z. Zheng, Y. Wang, W. Geng, and F. Zhang, *J.Phys.Chem. Solids*, 76 (2015) 88-93.
10. R. Ghosh and D. Basak, *Appl. Surf. Sci.*, 255 (2009) 7238-7242.
11. M. H. Mamat, M. Z. Sahdan, Z. Khusaimi, A. Z. Ahmed, S. Abdullah, and M. Rusop," *Opt. Mater.*, 32 (2010) 696-699.
12. P. P. Sahay and R. K. Nath, *Sens. Actuator B,* 134 (2008) 654-659.
13. Y. Caglar, *J. Alloys Comp,*. 560 (2013) 181-188.
14. R. Elilarassi and G. Chandrasekaran, *Mater. Sci. Semicond. Processing*. 14 (2011) 179- 183.
15. G. J. Lee, *J.Nanosci.Nanotechnol.,* 6 (2011) 511-517.
16. K. A. Wahid, W. Y. Lee, H. W. Lee, A. S. Teh, D. C. S. Bien, and I. A. Azid, *Appl. Surf. Sci*., 283 (2013) 629-635.
17. B. İkizler and S. M. Peker, *Thin Solid Films*. 558 (2014) 149-159.
18. D. Fang, P. Yao, and H. Li, *Ceram. Int,*. 40 (2014) 5873-5880.
19. J. Zhang and W. Que, *Sol. Energy Mater. Sol. Cells,* 94 (2010) 2181-2186.
20. A. N. Mallika, A. Ramachandra Reddy, K. Sowri Babu, C. Sujatha, and K. Venugopal Reddy, *Opt. Mater.*, 36 (2014) 879-884.
21. B. Shouli, C. Liangyuan, L. Dianqing, Y. Wensheng, Y. Pengcheng, L. Zhiyong, C. Aifan, and C. C. Liu, *Sens. Actuators B,* 146 (2010) 129-137.
22. C.-C. Ting, C.-H. Li, C.-Y. Kuo, C.-C. Hsu, H.-C. Wang, and M.-H. Yang, *Thin Solid Films*. 518 (2010) 4156-4162.
23. S. Bai, T. Guo, D. Li, R. Luo, A. Chen, and C. C. Liu, *Sens. Acuators B,* 182 (2013) 747-754.
24. Z. Ben Ayadi, L. El Mir, K. Djessas, and S. Alaya, *Thin Solid Films*, 517 (2009) 6305- 6309.